Journal of Magnetic Resonance **138,** 98–106 (1999)
Article ID jmre.1999.1726, available online at http://www.idealibrary.com on IDEAL®

Structural Parameters from ^{19}F Homonuclear Dipolar Couplings, Obtained by Multipulse Solid-State NMR on Static and Oriented Systems

Stephan L. Grage and Anne S. Ulrich[1]

Institut für Molekularbiologie, Friedrich-Schiller-Universität Jena, Winzerlaer Str. 10, 07745 Jena, Germany

Received August 19, 1998; revised November 25, 1998

Local macromolecular structure can be determined by solid-state NMR measurements of weak dipolar couplings between selectively labeled groups. The nonperturbing use of ^{2}H, ^{13}C, or ^{15}N in biological systems, however, faces drawbacks in terms of a low sensitivity and a comparatively short distance range relative to ^{1}H. To extend these limitations, we illustrate the use of ^{19}F as an alternative NMR probe. The Carr–Purcell–Meiboom–Gill (CPMG) multipulse sequence was adapted here to measure homonuclear dipolar couplings between two fluorine labels in static samples at 470 MHz. Two lipids (4,4-DMPC-F_2, and a difluorinated sterol), which are arranged in liquid crystalline bilayers, serve as models to assess the scope of the technique. In these ^{19}F-background-free biological samples, weak couplings down to 100 Hz could be resolved directly from the splitting of the pure dipolar powder lineshape, and ^{1}H-decoupling was not required. Order parameters were determined for the anisotropic motion of the lipids, consistent with their expected behavior in the membrane. Besides measuring the distance-dependent term of the dipolar coupling in powder samples, we have also used oriented membranes to extract additional angular information from the dipolar anisotropy. The strategy presented here thus has the potential to obtain not only the internuclear distance between two labels, but also their angular orientation in the sample, provided the molecules are aligned as a membrane or a fiber. © 1999 Academic Press

Key Words: **solid state ^{19}F-NMR; homonuclear dipolar coupling; CPMG multipulse; uniaxially oriented sample; membrane lipid.**

INTRODUCTION

Solid-state NMR is a powerful tool for the structural analysis of complex systems that do not crystallize, such as biological membranes or fibrous samples (*1–4*). Unlike solution-state NMR, this approach is not intrinsically limited by the size or aggregation state of the molecules, but low resolution and poor sensitivity represent major problems in current biological applications. While solution-state NMR is able to resolve and assign all protons and other nuclei in uniformly labeled proteins of $\lesssim$30 kDa, equivalent techniques have not yet been established for large molecular complexes (*5*). Significant progress has been made in obtaining well-resolved solid-state NMR spectra of uniformly labeled and oriented membrane proteins (*6*), but most applications still rely on specifically labeled samples and yield only a single local structural parameter at a time. For example, it is possible to measure the internuclear distance between two labels, the torsion angle between two such groups, or the orientation of a molecular segment with respect to the membrane normal (see Fig. 1). To collect a comprehensive three-dimensional data set that way, many labeled samples have to be prepared and analyzed. Since the sensitivity of conventional isotope labels, such as ^{13}C, ^{15}N, and ^{2}H, is much lower than that of protons, the availability of biological material and instrument time may represent an additional problem. Here, we suggest an NMR strategy that is capable of extending both limitations. Sensitivity is enhanced by using ^{19}F as a probe, and the information content of a single sample can in principle be doubled by measuring both the distance between and the internuclear orientation of two labels in an oriented sample.

In terms of sensitivity, the ^{19}F nucleus (spin $\frac{1}{2}$) offers a unique potential for biological solid-state NMR. Its gyromagnetic ratio γ is higher than that of conventional labels, yielding 83% of the sensitivity of protons, whereas ^{13}C, ^{2}H, or ^{15}N only reach 1.6, 1.0, or 0.1%, respectively (*7*). Equally important, the dipolar interactions of ^{19}F reach out much farther into the distance. For example, assuming a resolution of 30 Hz, it should be possible to measure ^{19}F–^{19}F distances up to 16 Å, as opposed to 6 Å between two ^{13}C labels (*2*). Furthermore, the broad chemical shift range of ^{19}F (up to 400 ppm) provides excellent resolution, and no natural abundance background has to be considered in biological systems. Of course, the labeling site in a biological molecule has to be carefully selected to avoid structural or functional perturbations. Studies on fluorinated lipids, like the ones used here, have revealed only minor side effects when a chain segment is labeled (*8*). Their order parameters are similar to those of deuterated analogues, and changes in the phase transition temperature are not severe (*9*). The van der Waals radius of fluorine (1.4 Å) is not too different from that of hydrogen (1.2 Å), although electronegativity ef-

[1] To whom correspondence should be addressed; E-mail: ulrich@molebio.uni-jena.de.

1090-7807/99 $30.00

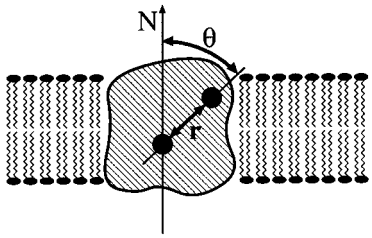

FIG. 1. For solid-state NMR analysis, a pair of labels is introduced into a membrane-bound molecule. Their internuclear distance r and the orientation θ of the internuclear vector with respect to the membrane normal (**N**) can be determined from the dipolar coupling.

fects have to be considered. Many fluorinated proteins have been investigated in terms of their structure and function, and in most cases the perturbation of the system was negligible (*10–13*). The main reason that solid-state ^{19}F-NMR has not yet found a more widespread application appears to be technical: The need for high-power ^{1}H-decoupling at a frequency close to that of ^{19}F (within 6%), together with a wide chemical shift range at high magnetic field strength, place stringent demands on filtering, probe design, and spectrometer hardware (*14*). Nevertheless, ^{1}H-decoupled ^{19}F high-resolution solid-state experiments have been successfully performed (*15, 16*). Here, we show the feasibility of suppressing the ^{19}F chemical shift in static experiments even on a high-field spectrometer, and of resolving ^{19}F–^{19}F dipolar interactions even without ^{1}H-decoupling.

Among previous biological ^{19}F-NMR applications, there are several examples where fluorine homo- or heteronuclear dipolar interactions have been used to analyze local macromolecular structure. For example, Schaefer *et al.* have measured internuclear ^{19}F–^{13}C distances in frozen enzymes (*17, 18*), and heteronuclear couplings from ^{19}F to ^{31}P, ^{13}C, or ^{15}N have been used for structural studies on various polymers and biological systems (*19–22*). Many years back, Post *et al.* determined segmental order parameters from the homonuclear dipolar coupling between geminal ^{19}F-labels on acyl chains in liquid crystals and membranes (*8, 23–26*). In each case it was necessary to isolate the desired dipolar interaction from all other interactions, such that the coupling strength could be interpreted in terms of internuclear distance or orientation. To this aim, a variety of solid-state NMR experiments have been developed over recent years, which can be distinguished mainly in terms of the mode of line-narrowing and the necessary sample geometry.

1. Intramolecular distances (see Fig. 1) can be determined from the dipolar coupling Δ, which depends on the distance r as $\Delta \sim 1/r^3$. Prominent homo- and heteronuclear techniques such as rotational resonance (RR) and REDOR have been used to measure *weak dipolar couplings* with high accuracy (*2, 4, 27–29*). These methods employ magic angle spinning to initially average all anisotropic interactions, and the desired dipolar interaction is then reintroduced by specific recoupling schemes.

2. *Strong dipolar interactions* have been resolved from static powder samples by coherent averaging in spin space rather than in real space. Nutation spectroscopy, for example, employs cw high-power RF irradiation to extract the homonuclear dipolar spectrum of a labeled spin pair in the shape of a Pake pattern (*30, 31*). Similarly, multipulse sequences such as the Carr–Purcell–Meiboom–Gill (CPMG) experiment can be used to selectively average chemical shift and heteronuclear interactions, while leaving the homonuclear dipolar coupling unaffected (*32–36, 50*). Heteronuclear dipolar couplings can be revealed in analogous double resonance experiments such as SEDOR (*29, 37, 38*).

3. In a different kind of structural approach, the *anisotropy of the dipolar interaction* can be used to determine the orientation angle, θ, of two nuclei with respect to the static magnetic field direction (see Fig. 1). For this, a uniaxially oriented sample has to be prepared by spreading a membrane film onto glass plates, or by stretching a fiber (*39, 40*). Instead of selectively averaging unwanted interactions, a narrow contribution from the full anisotropy range is selected by aligning the molecules. This kind of resolution enhancement, like the suppression of undesired interactions above, enables the determination of the dipolar splitting Δ. Provided the internuclear distance r is known, θ can then be readily obtained from $\Delta \sim \frac{1}{2}(3\cos^2\theta - 1)$. In membrane-bound peptides, complete orientations of the backbone and side chains have been determined that way (*3, 41*).

Given the dependence of the dipolar coupling on both the distance and the internuclear angle between a pair of nuclei, it should in principle be possible to obtain both parameters. For this, it is necessary to combine a *static method* (category 2) with an *oriented system* (category 3), provided that *weak couplings* are still accessible (which is possible so far only with the methods in category 1). Such an approach appears hopeful in the case of ^{19}F, because it possesses strong couplings and no natural-abundance background. Especially the natural-abundance background of biological isotopes often prohibits the resolution of weak couplings.

THEORETICAL BACKGROUND

Combination of Distance and Orientation Measurements

The various experiments discussed above address either the distance or the angular dependence of the dipolar coupling. Here we propose a strategy to determine the values of both r and θ from the homonuclear dipolar coupling Δ of a spin pair (Fig. 1), provided the coupling is not narrowed by molecular motion on the time scale of the NMR experiment. First, the internuclear distance r is measured from the splitting of the dipolar powder spectrum of a nonoriented sample, where $\theta = 90°$. Then, knowing r, the dipolar splitting of an oriented sample reveals the angle θ. Alternatively, r and θ can also be determined from a single oriented sample by varying its align-

ment in the external magnetic field (*42*). The technique used in this study to measure the dipolar coupling is based on the CPMG sequence (*32, 33*), which has already been successfully applied to determine internuclear distances and to evaluate motionally averaged order parameters (*23, 24, 26, 34, 35*). Oriented samples of fluorinated lipid bilayers have also been used previously for solid-state NMR investigations (*25*). However, to our knowledge measurements of homonuclear dipolar couplings have not yet been combined with oriented systems.

Homonuclear Dipolar Interaction

Several interactions contribute to the Hamiltonian H of a dilute spin pair $\mathbf{I}_1$ and $\mathbf{I}_2$ in the rotating frame:

$$H = H_{CS} + H_{IS} + H_{II}. \quad [1]$$

The dominant ones are the chemical shift H_{CS}, the heteronuclear dipolar coupling H_{IS}, and the homonuclear dipolar coupling H_{II}:

$$H_{CS} = \omega_1 I_{z1} + \omega_2 I_{z2} \quad [2]$$

$$H_{IS} = \sum_k (a_{1k} I_{z1} S_{zk} + a_{2k} I_{z2} S_{zk}) \quad [3]$$

$$H_{II} = b_{12}(3 I_{z1} I_{z2} - \mathbf{I}_1 \mathbf{I}_2), \quad [4]$$

where ω_1, ω_2, a_{jk}, and b_{jk} are constants. Structural information can be obtained from the homonuclear dipolar coupling, which depends on both the distance r and the internuclear orientation θ with respect to the external magnetic field. It leads to a splitting Δ in a pure dipolar spectrum:

$$\Delta = \frac{3 b_{12}}{2\pi} = \frac{3\gamma^2\hbar}{2\pi r^3}\left(\frac{3\cos^2\theta - 1}{2}\right). \quad [5]$$

Here, a Carr–Purcell–Meiboom–Gill (CPMG) sequence is used to reveal the pure homonuclear dipolar spectrum and to access the structural information that way.

The CPMG Sequence

Figure 2 shows the CPMG experiment, with an *xy*8 phase cycling scheme imposed on the multipulse train. (Details of the phase cycling modifications will be discussed below.) In the CPMG experiment, as originally invented by Carr and Purcell (*32*) and improved by Meiboom and Gill (*33*), a $\pi/2$ preparation pulse and a delay τ is followed by a series of refocusing π pulses, which are separated by 2τ and shifted 90° in phase with respect to the first pulse. The individual data points are sampled from the top of the echoes in every other 2τ window. When observed at these points in time, the spin system appears to evolve under an average Hamiltonian $\bar{H}$, where only the homonuclear dipolar interaction H_{II} contributes, while $H_{IS} + H_{CS}$ are coherently averaged to zero.

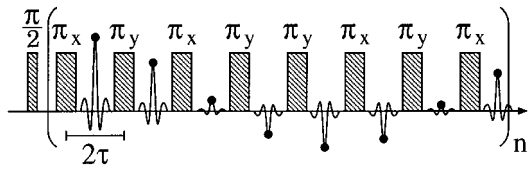

FIG. 2. The CPMG multipulse sequence (depicted here with an *xy*8 phase cycle) is used to extract the dipolar interaction in a static experiment. The chemical shift, heteronuclear dipolar couplings, and field inhomogeneities are refocused, while the homonuclear dipolar interaction evolves during the echo train. A Fourier transform of the oscillating echo amplitudes yields the pure dipolar spectrum.

Upon transferring the system into a suitable toggling frame (*43, 44*), the π pulses can be replaced by rotations of the Hamiltonian H with $R = \exp(i\pi I_y)$. This allows a stepwise definition of the Hamiltonian as H, $R^{-1}HR$, $R^{-1}R^{-1}HRR$, etc., in the respective first, second, etc., pulse window. Given that $RR = 1$, the system evolves alternately under H and $R^{-1}HR$. It follows from the dependence of the Hamiltonian on the spin variables that in the toggling frame, the effect of a π pulse is to invert the sign of H_{CS} and H_{IS}, but not of H_{II}:

$$R^{-1} H_{CS} R = -H_{CS}, \quad [6]$$

$$R^{-1} H_{IS} R = -H_{IS}, \quad [7]$$

$$R^{-1} H_{II} R = H_{II}. \quad [8]$$

When the Hamiltonian is averaged over one cycle of length $\tau_c = 4\tau$, the homonuclear dipolar interaction remains unchanged as H_{II}, but H_{CS} and H_{IS} cancel:

$$\bar{H} = \frac{1}{4\tau}(2\tau H + 2\tau R^{-1} H R) = H_{II}. \quad [9]$$

When observed stroboscopically once per cycle, the spin system then evolves under the influence of the average Hamiltonian $\bar{H} = H_{II}$ (*43, 44*).

Alternatively, the CPMG sequence can be visualized in the rotating frame, where each π pulse has the effect of refocusing the chemical shift anisotropy H_{CS} and the heteronuclear dipolar coupling H_{IS}, as well as field inhomogeneities. A train of echoes is generated in the windows at times $k2\tau$, $k = 1, 2, 3, \ldots$. Since H_{II} is unaffected by the π pulses, the spin system will still evolve under the homonuclear dipolar interaction. Thus, the echo amplitudes $A(k2\tau)$ are modulated by H_{II}, and a Fourier transform of the oscillating echo intensities yields the pure dipolar spectrum.

For Hamiltonians that do not commute at all times, perturbation terms of higher order in τ_c add to the average Hamiltonian. They remain small, however, as long as $\|H\|\tau_c \ll 1$. If the two coupled nuclei possess different chemical shifts, then

$[H_{CS}, H_{II}] \neq 0$, and H no longer commutes at different times. This imposes a limitation on the use of the CPMG sequence for nuclei with large differences in chemical shift. In those cases, it is crucial to suppress the evolution of higher order perturbations by choosing a sufficiently short τ window time.

Compensation of Pulse Imperfections

In the original CPMG sequence, incomplete refocusing due to pulse imperfections rapidly leads to an accumulation of errors. These errors result in a loss of echo amplitude, but they can be partially compensated by recent phase cycling schemes (*35, 45*). We use *xy*8 and *xy*16 with cycle lengths of $\tau_c = 16\tau$ and $\tau_c = 32\tau$, respectively. (See Fig. 2 for the *xy*8 phase cycle.) To increase the spectral width, we sample the data points in every window between successive π pulses, rather than only once per cycle. As a consequence, however, even though errors in the echo amplitude do not accumulate, they are repeated after every cycle. This leads to a beat in the FID, which shows up in the spectrum in the form of "sidebands" at frequencies $\pm 1/\tau_c$, $\pm 2/\tau_c$, etc. To exclude such sidebands from the region of interest in the spectrum, a careful selection of τ and an appropriate choice of phase cycle version are recommended.

Scaling of the Dipolar Splitting by the Duty Cycle

RF irradiation by the pulses themselves can be considered as a contribution to the Hamiltonian. It has been shown that pulses with a finite length, t_w, reduce the actual dipolar interaction by a scaling factor of $(1 - D)$, where the duty factor is $D = t_w/2\tau$ (*34*). Throughout this work, we have defined the evolution period 2τ as the time from the middle of a π pulse to the middle of the next π pulse. With this definition, the scaling by $(1 - D)$ is mathematically equivalent to considering only the free window $(2\tau - t_w)$ as the dwell time during which dipolar evolution can take place. In all Fourier transformations we have taken the necessary scaling into account, according to the duty cycle used in the individual experiments. Hence, the factor of $(1 - D)$ arising from finite pulse width is compensated, and all spectra are plotted to show the true dipolar frequencies.

MATERIALS

The phospholipid 1-myristoyl-2-(4,4-[$^{19}F_2$]difluoromyristoyl)-*sn*-glycero-3-phosphocholine (DMPC-F_2), which carries two geminal fluorine labels in one chain, was a gift from Chien Ho, Carnegie Mellon University of Pittsburgh (*8, 25, 26*). The doubly fluorinated sterol diflucortolon-21-valerate (DFC) was a gift from Schering AG, Berlin.

To prepare multilamellar liposomes of DMPC-F_2, 10 mg of the dry lipid was hydrated with 20 μl ultrapure H_2O above its phase transition temperature, and the vesicles were homogenized by mechanical stirring and repeated freeze–thawing. A sample of 5% DFC in DMPC (w/w) was obtained the same way, after cosolubilizing 100 mg of total lipid in $CHCl_3$, drying under N_2, overnight under vacuum, and hydrating with 200 μl H_2O.

To prepare oriented samples, three glass plates with dimensions of 4 mm $\times$ 20 mm $\times$ 0.07 mm were thoroughly cleaned with $CHCl_3$, MeOH, and H_2O. A total of 3 mg of DMPC-F_2 was dissolved in 60 μl $CHCl_3$ and spread in 20-μl aliquots evenly over the central portions of the glass plates. They were dried overnight, and each plate was then hydrated to saturation by exposing the lipid film to H_2O steam over boiling water. The plates were rapidly placed face-down onto a base plate, to form a stack, with full humidity maintained. The stack was wrapped in cling film and inserted into a 5-mm NMR tube. Before the glass tube was sealed with epoxide resin, two pads of cotton, soaked with H_2O, were inserted next to the glass plates.

EXPERIMENTAL

The solid-state NMR measurements were carried out at a ^{19}F resonance frequency of 470 MHz on a Varian widebore spectrometer (Unity Inova), equipped with a high-power ^{19}F-amplifier (Creative Electronics, Northridge, CA). A 5 mm XC Quad-tuned (HFCX) variable angle spinning probe (Doty Scientific Instruments, Columbia, SC) was used without spinning. The $\pi/2$ pulse length was 2.4 to 6.8 μs, depending on the orientation of the sample coil in the magnetic field, which could be freely adjusted with a goniometer. Band-selective ^{1}H and ^{19}F filters (FSY Microwave, Inc., Columbia, MD) together with additional bandstop filters (Doty Scientific) were used to acquire ^{1}H-decoupled ^{19}F-spectra.

All measurements on DMPC-F_2 and DFC/DMPC mixtures were carried out at 35°C, where the lipid bilayers are in the liquid crystalline phase. The wideline spectra were acquired with 128–512 transients of the Hahn-echo experiment ($\pi/2$–τ–π–τ) with a pulse spacing of $\tau = 20$ μs and a recycle delay of 1 s. About 30 kHz proton decoupling was applied.

The dipolar spectra were obtained using the CPMG sequence with pulse spacings from $2\tau = 30$ to 200 μs, and varying lengths of the pulse train between 13 and 320 ms. The echoes were acquired in the windows between the π pulses at a sampling rate of 1 point/μs. Up to 4 raw data points at the echo top were averaged, and an FID analogue was then composed from these average echo amplitudes. About 1000 transients were accumulated for powder samples, and about 10,000 in the case of the oriented sample. The phase alternation of the magnetization in the successive windows was taken into account by software manipulation. The FID analogue was then converted into the dipolar spectrum via Fourier transform.

RESULTS AND DISCUSSION

The feasibility of the proposed ^{19}F-NMR CPMG strategy is evaluated here using two kinds of doubly labeled lipids for

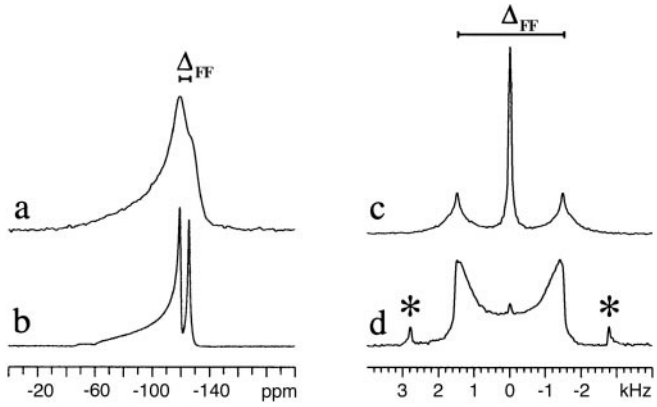

FIG. 3. The ^{19}F-NMR Hahn-echo spectrum of DMPC-F_2 multilamellar vesicles is dominated by the chemical shift anisotropy and broadened by ^{1}H-interactions (a, 128 transients). Proton decoupling resolves the dipolar coupling of the two geminal fluorines of $\Delta_{FF} = 3.1$ kHz (b, 512 transients). The CPMG experiment reveals the pure dipolar spectrum (c, d, train of 256 pulses with $2\tau = 50$ μs, ~1000 transients). The spectrum obtained with the original CPMG sequence (c), however, is significantly distorted. Application of the *xy*8 phase cycle improves the powder lineshape (d), despite the appearance of sideband-like artifacts (marked with *).

which the dipolar couplings and other structural parameters are known. The two lipids, DMPC-F_2 and DFC, possess different properties in terms of dipolar coupling strength and chemical shift dispersion. Hence, the capabilities of the CPMG approach can be examined under different conditions. DMPC-F_2 (averaged by long-axial rotation) has two magnetically equivalent ^{19}F nuclei coupled by a reasonably strong dipolar interaction. In contrast, the chemical shifts of the two ^{19}F substituents on any one DFC molecule (also motionally averaged) are well separated by a chemical shift difference much larger than the residual dipolar coupling.

Revealing the Dipolar Powder Spectrum of DMPC-F_2

The standard ^{19}F NMR Hahn-echo powder spectrum of DMPC-F_2 (Fig. 3a) is dominated by the chemical shift anisotropy, and further broadened by homo- and heteronuclear dipolar interactions. At 470 MHz, moderate ^{1}H-decoupling of 25 kHz is sufficient to resolve the strong homonuclear dipolar coupling between the two geminal fluorine labels, as seen in the lower spectrum (Fig. 3b). The splitting of $\Delta_{FF} = 3.1$ kHz at the high-field edge compares well (within 7%) with the dipolar coupling reported by Ho *et al.* on the same compound and at the same temperature (*8*). In these earlier studies, which were performed at 282 MHz without ^{1}H-decoupling, the ^{19}F–^{19}F coupling had to be extracted from the unresolved spectrum by lineshape deconvolution (*25*).

A CF_2-group that is rigid on the NMR time scale would give rise to a splitting of $\Delta_0 = 15.4$ kHz in the powder spectrum (*8, 25*). The reduced value of 3.1 kHz measured here is due to the long-axial rotation and further chain fluctuations of the lipid molecule, which are described by an order parameter $S_{FF} = \Delta_{FF}/\Delta_0$. In good agreement with previous reports on DMPC-F_2 ($S_{FF} = 0.19$), we evaluate S_{FF} as 0.20, which is also reasonably similar to the order parameter of the deuterated DMPC analogue ($S_{CD} = 0.22$) (*8, 26*). Knowing the order parameter, it follows from the total width of the spectrum (Fig. 3a, 3b) that the underlying anisotropy of the axially symmetric chemical shift tensor of a straight all-*trans* CF_2 chain segment (which only undergoes fast rotation about the long lipid axis) is 169 ± 1 ppm, and its isotropic position is at 101 ± 1 ppm relative to $CFCl_3$.

The pure dipolar ^{19}F spectrum of DMPC-F_2, measured with the CPMG sequence, is shown in Fig. 3c. While the Hahn-echo spectrum is dominated by the chemical shift interaction and heteronuclear dipolar broadening (Fig. 3a), these interactions are successfully suppressed here. We emphasize that no ^{1}H-decoupling was necessary to resolve the dipolar splitting in this multipulse experiment. Nevertheless, the lineshape obtained here at 470 MHz with the conventional CPMG pulse train is significantly distorted, especially by a strong artifact in the center (Fig. 3c). In a previous CPMG study on DMPC-F_2 at a lower field strength of 40 MHz, where the chemical shift range is much narrower, such lineshape distortions were insignificant (*26*).

Using a compensated CPMG version, CPMG-*xy*8, the dipolar spectrum of DMPC-F_2 could be significantly improved, as seen in Fig. 3d. The *xy*8 phase cycling scheme prevents the accumulation of errors due to imperfect π pulses during the pulse train, which becomes especially important for measuring weak dipolar interactions in the presence of large offset dispersion (*35, 45*). The duration of the dipolar oscillation in time is significantly improved, and a much higher spectral resolution is gained. Hence, on a high-field spectrometer the compensated CPMG-*xy*8 scheme helps to obtain undistorted lineshapes and accurate values for the dipolar coupling. On the other hand, the improvements are accompanied by sideband-like spikes, which are introduced by the repeat rate of the phase cycle. Using *xy*16 instead of *xy*8 did not lead to any further improvement, but instead yielded more sidebands.

The dipolar CPMG-*xy*8 spectrum in Fig. 3d has a peak-to-peak splitting of $\Delta_{FF} = 3.0$ kHz, which is the same as in the Hahn-echo spectrum (Fig. 3b) within experimental error. A series of multipulse experiments was carried out with different duty cycles D between 2.5 and 33% to evaluate the validity of our scaling procedure. The splitting Δ_{FF} was found to depend linearly on the duty cycle D, and extrapolation to $D = 0$ confirmed a dipolar splitting of $\Delta_{FF} = 3.1$ kHz (data not shown). The scaling procedure, as described in the theory section, thus appears to be sufficient here. The dipolar spectra in Fig. 3 were acquired with a mid-to-mid pulse spacing of $2\tau = 50$ μs. Reasonable dipolar spectra are also obtained with longer pulse spacings, but the intensity decreases with increasing τ (data not shown). While short τ is a desirable option here, it will become crucial in the study of DFC to be discussed below.

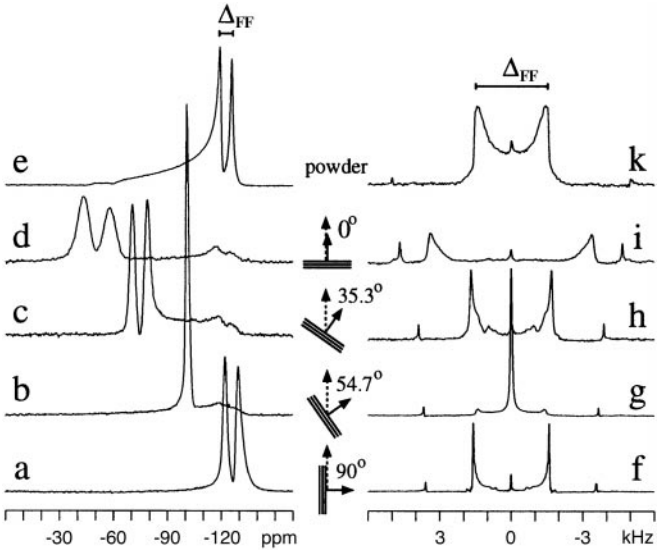

FIG. 4. ^{19}F-NMR of oriented DMPC-F_2 membranes (<3 mg lipid), aligned at various tilt angles α between the membrane normal and the spectrometer field. Both the ^{1}H-decoupled Hahn-echo spectra (a–d, 2048 transients) and the CPMG-*xy*8 spectra (f–i, train of 512 pulses with $2\tau = 40$ μs, ~10,000 transients) reveal the orientation-dependent dipolar splittings. The use of CPMG leads to a narrowing of the effective linewidth, as seen for example by comparison of the oriented spectra at $\alpha = 90°$, from 1.2 kHz (a) to <50 Hz (f). The dipolar splittings and the CSA range of the oriented lineshapes are about 10% larger than expected from the powder spectra (e, k), because of bilayer undulations. The outermost spikes in the CPMG-*xy*8 spectra are sideband artifacts due to the phase cycling.

Oriented DMPC-F_2 Bilayers

In a disordered sample all molecular orientations contribute to the powder spectrum. Since the splitting Δ_{FF} represents those interactions that are aligned perpendicular to the external magnetic field, the corresponding angle is $\theta = 90°$. Equation [5] can thus be used to calculate the internuclear distance r in a static molecule, or the order parameter S_{FF}, which is analogous to r in a motionally averaged lipid. Up to this point, only a single structural parameter is available. In the case of a static molecule, however, it would also be structurally relevant to determine the angle θ of the ^{19}F–^{19}F internuclear vector with respect to the membrane normal. Likewise, in a motionally averaged molecule or molecular segment, it may be worthwhile to know the tilt angle of the axis of averaging. Hence, an independent structural parameter can be obtained from an additional CPMG experiment of the same labeled compound, prepared as a uniaxially oriented sample and measured with its axis when parallel to the external magnetic field. The feasibility of this approach is evaluated here using DMPC-F_2, for which the angle between the membrane normal and the rotation axis is known to be zero. The oriented sample is also used to demonstrate the sensitivity and the reduction in linewidth that can be achieved by CPMG.

^{19}F-NMR Hahn-echo spectra of oriented DMPC-F_2 bilayers are shown in Fig. 4a–4d, acquired at different tilt angles α of the sample normal with respect to the external magnetic field. The powder spectrum is depicted in Fig. 4e for comparison. Moderate ^{1}H-decoupling was applied to resolve the splittings. In each oriented spectrum the pair of narrow lines arises from well-aligned membranes, and there is only a minor contribution of <10% from disordered material. Both the splittings $\Delta_{FF}(\alpha)$ and their chemical shift positions vary with $\frac{1}{2}(3\cos^2\alpha - 1)$. This axially symmetric behavior shows that $\alpha = \theta$, thus confirming the rotational averaging of the lipid molecules around an axis parallel to the membrane normal.

Remarkably, the spectral range covered by the oriented spectra (Fig. 4a–d) is found to be about 10% larger than the full width of the powder spectrum (Fig. 4e). Similarly, the dipolar splitting is 3.4 kHz for the oriented sample at $\alpha = 90°$, while the corresponding value is 3.1 kHz for the powder sample (Fig. 4a). The respective order parameters are $S_{FF} = 0.22$ and $S_{FF} = 0.20$. These differences suggest that the two samples differ slightly in terms of the motional averaging experienced by the lipids. However, we note that the small powder contribution in the oriented sample (Fig. 4b–d) occupies the same spectral position as in the designated powder spectrum (Fig. 4e), and therefore possesses to the same order parameter. This observation suggests that both samples have the same saturating hydration level, and that they do not differ in terms of composition, local heating effects, or lipid hydrolysis. Instead, we attribute the different order parameters to the motional contribution of bilayer undulations, which are known to be reduced for membranes oriented between glass plates (*46*).

The pure ^{19}F dipolar spectra of the oriented DMPC-F_2 sample are shown in Fig. 4f–4i. The chemical shift interaction, heteronuclear couplings, and field inhomogeneities are suppressed by the CPMG multipulse sequence with *xy*8 phase cycling. The orientation-dependent dipolar splittings in this series of spectra are in good agreement with the values obtained from the Hahn-echo spectra (Fig. 4a–4d): 6.8, 3.4, 0.0, and 3.2 kHz for $\theta = 0°$, 35.3°, 54.7°, and 90°, respectively. Again, the splittings of the oriented membrane sample (Fig. 4f–4i) are 10% larger than of the powder sample (Fig. 4k) or of the residual powder contribution from disordered lipids in the oriented bilayers (Fig. 4g). More significantly at this point, we note the dramatic reduction in linewidth in the oriented CPMG spectrum of DMPC-F_2. The linewidth of 1.2 kHz in the Hahn-echo spectrum at $\alpha = 90°$ (Fig. 4a) is reduced to below the resolution limit of 50 Hz in the corresponding CPMG spectrum (Fig. 4f). To provide a comparison of sensitivity, roughly four times as many transients were acquired for a CPMG than for a Hahn-echo of the same sample, to reach a similar S/N. Therefore, the one-dimensional CPMG analysis is highly efficient compared to other time-incremented approaches for measuring weak dipolar couplings.

Two-Dimensional Dipolar Spectroscopy

In some applications to biopolymers it might be favorable to introduce several ^{19}F pairs into a molecule to increase the

information content accessible from one sample. In other cases, multiple spin pairs might be inevitable, for example, when fluorine labels are incorporated biosynthetically into proteins. Therefore, an extension of the CPMG approach into two dimensions may help to separate any pairwise couplings between distinct fluorine nuclei. The most straightforward approach to including a second wideline dimension is illustrated in Fig. 5. This 2D spectrum of DMPC-F_2 was obtained by acquiring a complete FID after each incremented *xy*8 dipolar evolution period, instead of monitoring the single echo in each window of an *xy*8 pulse train. The resulting spectrum contains the chemical shift in one dimension and the dipolar coupling in the other. It can be considered as the homonuclear equivalent of a dip-shift or separated local field experiment (*47, 48*). The spectral intensity is somewhat underrepresented at the low-field edge of the direct dimension (Fig. 5), but the dipolar coupling is in good agreement with the 1D data shown above.

Weak Dipolar Coupling in DFC

To investigate a second, more challenging compound than DMPC-F_2, the doubly fluorinated sterol DFC (see Fig. 6) was embedded at 5% in a DMPC membrane matrix. In this case, the intramolecular dipolar coupling is not so readily resolved because the two fluorines in DFC possess distinctly different chemical shift ranges. Moreover, the comparatively weak dipolar coupling of the more distant ^{19}F nuclei is further reduced by motional averaging of the molecule in the liquid crystalline bilayer.

As shown in Fig. 6a, the Hahn-echo is not able to resolve the weak dipolar coupling in DFC, even with ^1H-decoupling. Note that the two signals in the spectrum represent the two chemically distinct ^{19}F nuclei, rather than their dipolar splitting. Using the CPMG experiment with *xy*16, their dipolar coupling of 100 Hz is well resolved without ^1H-decoupling (Fig. 6b–6f). From molecular dynamics simulation of the rigid sterol, we estimate an internuclear ^{19}F–^{19}F distance of 4.4 Å in DFC, which corresponds to a static coupling constant of 1.9 kHz. Assuming a fast uniaxial rotation of the DFC molecule about the membrane normal, the averaged dipolar coupling of 100 Hz would correspond to a tilt angle of ~53° for the internuclear ^{19}F–^{19}F vector with respect to the rotation axis. Likewise, ^2H-NMR studies of deuterated cholesterol in model membranes yielded a similar orientation, close to the magic angle, for the comparable bond vector C_6–^2H (*49*). However, we note a dramatic reduction in the Hahn-echo linewidth (Fig. 6a) of both ^{19}F substituents, when compared to the spectral width of the crystalline substance (data not shown). Therefore, it is likely that DFC experiences a high degree of motional freedom in the bilayer and is able to tumble with a comparatively low order parameter, approaching an isotropic average. Diffusion over curved surfaces can be excluded as the predominant narrowing mechanism, as the DFC-containing vesicles were estimated to be at least several micrometers in size by electron microscopy.

A series of dipolar spectra was acquired with pulse spacings 2τ between 200 and 30 μs (Fig. 6b–6f). For long window delays, only a weak unresolved lineshape is obtained. A short window of $2\tau < 50$ μs is crucial to separate the two peaks of the powder spectrum. In the case of DFC, the chemical shift interaction no longer commutes with the homonuclear dipolar interaction, and higher order terms arise in the average Ham-

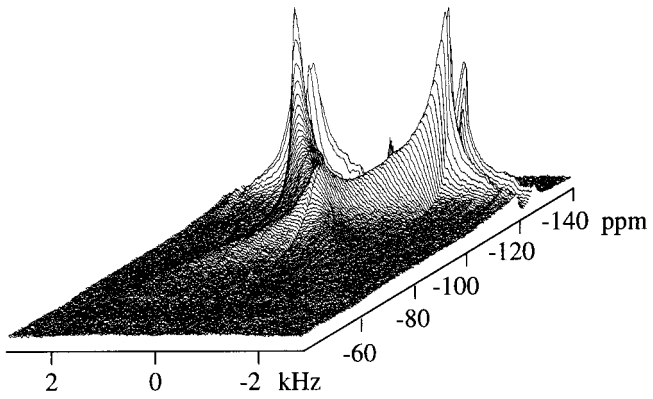

FIG. 5. ^{19}F-NMR CPMG-xy8 spectra of DMPC-F_2 are extended into a second wideline dimension. For this, a complete FID was acquired with 30 kHz proton decoupling, following an incremented CPMG pulse train (512 increments, acquired after every other 50 μs window, 160 transients).

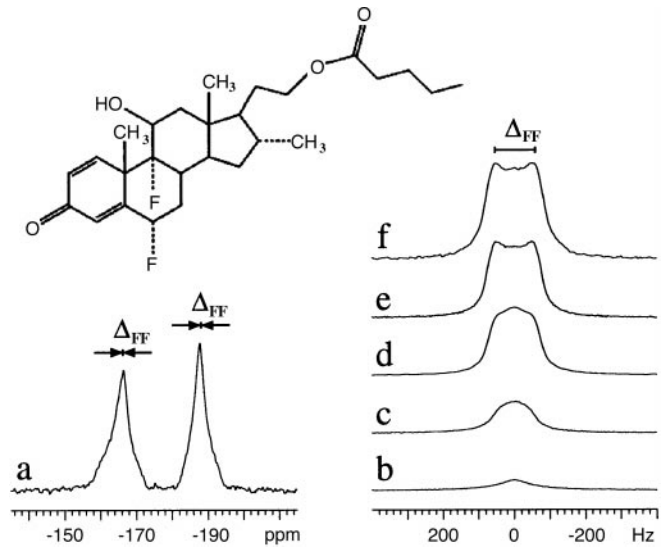

FIG. 6. Diflucortolon-21-valerate (DFC), dissolved at 5% in DMPC bilayers, was studied as a model compound with weak dipolar coupling. The sterol contains two chemically distinct ^{19}F labels (see insert). They give rise to two distinct signals in the Hahn-echo spectrum (a), and their weak dipolar coupling is not resolved. Coherent averaging by CPMG-*xy*16, however, reveals their dipolar coupling of $\Delta_{FF} = 100$ Hz (f). The variation of the mid-to-mid pulse spacing, $2\tau = 200, 100, 50, 40, 30$ μs (b–f), demonstrates the importance of short windows to resolve weak couplings in the presence of large chemical shift differences. The CPMG pulse trains consisted of 640 (for $2\tau = 200$ μs, b) to 5120 (for $2\tau = 30$ μs, f) pulses, and 256 transients were averaged in the Hahn-echo and ~1000 in the CPMG spectra.

iltonian. Spin dephasing and the resulting spectral distortions can only be suppressed by choosing sufficiently short windows in the CPMG multipulse train. The limiting value of 2τ is determined by the chemical shift difference of 10 kHz between any pair of coupled ^{19}F nuclei. That is, in order to be successfully refocused and suppressed, the chemical shift and other undesired interactions must not be allowed to evolve substantially within 2τ. The broad chemical shift range of ^{19}F indeed represents one of the major challenges to be faced with high-field spectrometers such as the one used here (470 MHz for ^{19}F). It also ought to be emphasized that the lack of a ^{19}F natural abundance background has made it possible to determine the weak dipolar coupling directly from the spectral lineshape, without having to resort to difference spectra or simulation procedures.

CONCLUSIONS

Current solid-state NMR investigations of biomolecules are often hampered by weak signal intensities and by the small number of structural parameters accessible from limited amounts of labeled material. We have illustrated here an NMR strategy to improve both situations.

First of all, ^{19}F labeling is superior to conventional labeling schemes in terms of sensitivity, distance range, and natural abundance background. Based on earlier reports, we have confirmed the feasibility of static ^{19}F CPMG experiments to determine weak dipolar couplings, even on a high-field spectrometer. Pure dipolar spectra can thus be rapidly obtained in a 1D experiment, using standard hardware with a single ^{19}F channel and without ^{1}H-decoupling, provided a Teflon-free probe is available. The comparatively high demands on the hardware in terms of pulse widths and power-handling capabilities are met by commercial probes and amplifiers. Difficulties due to the wide chemical shift range of ^{19}F are within scope for labeled biological samples. Furthermore, using a combination of oriented samples and multipulse techniques, we have illustrated a strategy to reveal both the distance and the orientation dependence of the dipolar interaction at once.

We have evaluated the ^{19}F-NMR approach using fluorinated lipids in liquid crystalline bilayers as model membranes, which can be readily prepared as oriented samples. The long-axial rotation of the molecules in these examples has the advantage of partially averaging the chemical shifts and heteronuclear couplings, which enhances the efficiency of the multipulse narrowing. The homonuclear ^{19}F dipolar coupling is reduced as well, which has made the strong coupling of DMPC-F_2 more conveniently accessible, but on the other hand has led to a very small residual splitting in the case of DFC. The spectral distortions and the line broadening encountered here could be avoided by applying a phase-compensated version of CPMG, and by choosing very short pulse spacings. Using oriented DMPC-F_2 samples, we have shown that CPMG has the ability to reduce an effective 1.2 kHz linewidth to below 50 Hz. In DFC, a 100 Hz splitting could be resolved in the presence of a 10 kHz chemical shift difference.

These examples have demonstrated the success of static dipolar ^{19}F experiments in comparatively mobile molecules, i.e., lipids in liquid crystalline bilayers. Because of their long-axial rotation, one of the two accessible structural parameters is trivial in these examples, as it defines the long axis of averaging. In a static molecule, however, it becomes structurally relevant to determine both the distance and the orientation of the ^{19}F–^{19}F internuclear vector. Therefore, to apply the suggested strategy to its full extent, it will be desirable to extend the approach to systems without motional averaging, such as membrane proteins or even crystalline solids. As with other solid-state NMR techniques, the time scale of spin diffusion and T_2 relaxation will determine the limitations of this static ^{19}F approach (*17*). We are currently evaluating the ability of CPMG to resolve ^{19}F dipolar splittings in crystalline model compounds, which appears to be feasible under certain conditions.

ACKNOWLEDGMENTS

The authors thank Chien Ho for the kind gift of DMPC-F_2 and gratefully acknowledge Schering AG and Ferdinand Männle for providing the DFC. We also thank Helmut Meyer (Univ. Jena) for the characterization of our samples by electron microscopy, and Reinhard Ulrich (TU Harburg), Matthias Grüne (Univ. Würzburg), Doty Scientific Inc., and Dave Cross (Varian, Darmstadt) for their invaluable technical advice. This work was supported by the Deutsche Forschungsgemeinschaft within SFB 197 (TP B13), and by a graduate fellowship from the Freistaat Thüringen.

REFERENCES

1. A. Watts, A. S. Ulrich, and D. A. Middleton, Solid-state NMR studies of membrane proteins, *Mol. Membr. Biol.* **12,** 233–246 (1995).
2. S. O. Smith, K. Aschheim, and M. Groesbeek, Magic angle spinning NMR spectroscopy of membrane proteins, *Quart. Rev. Biophys.* **29,** 395–449 (1996).
3. S. J. Opella, NMR and membrane proteins, *Nature Struct. Biol., NMR supplement,* 845–848 (1997).
4. R. G. Griffin, Dipolar recoupling in MAS spectra of biological solids, *Nature Struc. Biol., NMR supplement,* 508–512 (1998).
5. H. Patzelt, A. S. Ulrich, P. Düx, H. Egbringhoff, J. Ashurst, H. Oschkinat, and D. Oesterhelt, Structural investigations on native bacteriorhodopsin in detergent micelles by NMR spectroscopy, *J. Biomol. NMR* **10,** 95–106 (1997).
6. Y. Kim, K. Valentine, S. J. Opella, S. L. Schendel, and W. A. Cramer, Solid-state NMR studies of the membrane-bound closed state of the colicin E1 channel domain in lipid bilayers, *Prot. Sci.* **7,** 342–348 (1998).
7. J. N. S. Evans, "Biomolecular NMR Spectroscopy," p. 7, Oxford Univ. Press, Oxford, UK (1995).
8. S. R. Dowd, V. Simplaceanu, and C. Ho, Fluorine-19 nuclear magnetic resonance investigation of fluorine-19-labeled phospholipids. 2. A line-shape analysis, *Biochemistry* **23,** 6142–6146 (1984).
9. E. Oldfield, R. W. K. Lee, M. Meadows, S. R. Dowd, and C. Ho, Deuterium NMR of specifically deuterated fluorine spin probes, *J. Biol. Chem.* **255,** 11652–11655 (1980).

10. E. Y. Lau and J. T. Gerig, Effects of fluorine substitution on the structure and dynamics of complexes of dihydrofolate reductase (*Escherichia coli*), *Biophys. J.* **73,** 1579–1592 (1997).
11. M. Bouchard, C. Paré, J.-P. Dutasta, J.-P. Chauvet, C. Gicquaud, and M. Auger, Interaction between G-Actin and various types of liposomes: A ^{19}F, ^{31}P, and ^{2}H nuclear magnetic resonance study, *Biochemistry* **37,** 3149–3155 (1998).
12. M. A. Danielson and J. J. Falke, Use of ^{19}F NMR to probe protein structure and conformational changes, *Annu. Rev. Biophys. Biomol. Struct.* **25,** 163–195 (1996).
13. J. T. Gerig, Fluorine NMR of proteins, *Prog. NMR Spectr.* **26,** 293–370 (1994).
14. S. A. Carss, U. Scheler, and R. K. Harris, ^{19}F NMR of proton-containing solids, *Magn. Reson. Chem.* **34,** 63–70 (1996).
15. R. K. Harris and P. Jackson, High-resolution fluorine-19 magnetic resonance of solids, *Chem. Rev.* **91,** 1427–1440 (1991).
16. J. M. Miller, Fluorine-19 magic-angle spinning NMR, *Prog. NMR Spectr.* **28,** 255–281 (1996).
17. L. McDowell, M. Lee, R. A. McKay, K. S. Anderson, and J. Schaefer, Intersubunit communication in tryptophan synthase by carbon-13 and fluorine-19 REDOR NMR, *Biochemistry* **35,** 3328–3334 (1996).
18. L. M. McDowell, S. M. Holl, S. Qian, E. Li, and J. Schaefer, Inter-tryptophan distances in rat cellular retinol binding protein II by solid-state NMR, *Biochemistry* **32,** 4560–4563 (1993).
19. L. M. McDowell and J. Schaefer, High-resolution NMR of biological solids, *Curr. Opin. Struct. Biol.* **6,** 624–629 (1996).
20. G. Tong, Y. Pan, M. Afeworki, M. D. Poliks, and J. Schaefer, Rotational-echo double-resonance NMR to observe the interfaces of heterogeneous polymer blends, *Macromol.* **28,** 1719–1720 (1995).
21. K. L. Wooley, C. A. Klug, K. Tasaki and J. Schaefer, Shapes of dendrimers from rotational-echo double-resonance NMR, *J. Am. Chem. Soc.* **119,** 53–58 (1997).
22. D. R. Studelska, C. A. Klug, D. D. Beusen, L. M. McDowell and J. Schaefer, Long-range distance measurements of protein binding sites by rotational-echo double-resonance NMR, *J. Am. Chem. Soc.* **118,** 5476–5477 (1996).
23. J. F. Post, E. E. J. de Ruiter, and H. J. C. Berendsen, A fluorine NMR study of model membranes containing ^{19}F-labeled phospholipids and an intrinsic membrane protein, *FEBS Lett.* **132,** 257–260 (1981).
24. J. F. M. Post, E. James, and H. J. C. Berendsen, Multipulse fluorine NMR experiments on lyotropic liquid crystals. I. Determination of order parameter tensor, *J. Magn. Reson.* **47,** 251–263 (1982).
25. M. Engelsberg, S. R. Dowd, V. Simplaceanu, B. W. Cook, and C. Ho, Nuclear magnetic resonance line-shape analysis of fluorine-19-labeled phospholipids, *Biochemistry* **21,** 6985–6989 (1982).
26. J. F. M. Post, B. W. Cook, S. R. Dowd, I. J. Lowe, and C. Ho, Fluorine-19 nuclear magnetic resonance investigation of fluorine-19-labeled phospholipids. 1. A multiple-pulse study, *Biochemistry* **23,** 6138–6141 (1984).
27. D. P. Raleigh, M. H. Levitt, and R. G. Griffin, Rotational resonance in solid state NMR, *Chem. Phys. Lett.* **146,** 71–76 (1988).
28. T. Gullion and J. Schaefer, Detection of weak heteronuclear dipolar coupling by rotational-echo double-resonance nuclear magnetic resonance, *Adv. Magn. Reson.* **13,** 57–83 (1989).
29. T. Terao, Structural measurements by solid-state NMR, *J. Mol. Struct.* **441,** 283–294 (1998).
30. C. S. Yannoni and R. D. Kendrick, NMR nutation spectroscopy: a method for determining molecular geometry in amorphous solids, *J. Chem. Phys.* **74,** 747–749 (1981).
31. C. S. Yannoni and T. C. Clarke, Molecular geometry of cis- and trans-polyacetylene by nutation NMR spectroscopy, *Phys. Rev. Lett.* **51,** 1191–1193 (1983).
32. H. Y. Carr and E. M. Purcell, Effects of diffusion on free precession in nuclear magnetic resonance experiments, *Phys. Rev.* **94,** 630–638 (1954).
33. S. Meiboom and D. Gill, Modified spin-echo method for measuring nuclear relaxation times, *Rev. Sci. Instrum.* **29,** 688–691 (1958).
34. M. Engelsberg and C. S. Yannoni, The determination of bond lengths in solids using the Carr–Purcell Sequence, *J. Magn. Reson.* **88,** 393–400 (1990).
35. M. J. Lizak, T. Gullion, and M. S. Conradi, Measurements of like-spin dipole couplings, *J. Magn. Reson.* **91,** 254–260 (1991).
36. K. Hirao, Y. Ishii, T. Terao, Y. Kishimoto, T. Miyatake, T. Ikariya, and R. Noyori, Solid-state NMR study of poly(phenylacetylene) synthesized with a rhodium complex initiator, *Macromol.* **31,** 3405–3408 (1998).
37. M. Emshwiller, E. L. Hahn, and D. Kaplan, Pulsed nuclear resonance spectroscopy, *Phys. Rev.* **118,** 414–424 (1960).
38. G. Buntkowsky, I. Sack, H. H. Limbach, B. Kling, and J. Fuhrhop, Structure elucidation of amide bonds with dipolar chemical shift NMR spectroscopy, *J. Phys. Chem.* **101,** 11265–11272 (1997).
39. T. Asakura, M. Minami, R. Shimada, M. Demura, M. Osanai, T. Fujito, M. Imanari, and A. S. Ulrich, ^{2}H-labeling of *Bombyx mori* silk fibers and their structural characterization by solid state ^{2}H-NMR, *Macromol.* **30,** 2429–2435 (1997).
40. A. S. Ulrich, I. Wallat, M. P. Heyn, and A. Watts, Re-alignment of the retinal chromophore in the M-state of bacteriorhodopsin, *Nature Struct. Biol.* **2,** 190–192 (1995).
41. R. R. Ketchem, B. Roux, and T. A. Cross, High-resolution polypeptide structure in a lamellar phase lipid environment from solid state NMR derived orientational constraints, *Structure* **5,** 1655–1669 (1997).
42. A. S. Ulrich and A. Watts, ^{2}H-NMR lineshapes of immobilized uniaxially oriented membrane proteins, *Solid State NMR* **2,** 21–36 (1993).
43. U. Haeberlen, High resolution NMR in solids, selective averaging, *in* "Advances in Magnetic Resonance," Suppl. 1 (J. S. Waugh, Ed.), Academic Press, New York (1976).
44. M. Mehring, "Principles of High Resolution NMR in Solids," Springer, New York (1983).
45. T. Gullion, D. B. Baker, and M. S. Conradi, New, compensated Carr-Purcell sequences, *J. Magn. Reson.* **89,** 479–484 (1990).
46. C. Glaubitz and A. Watts, Magic angle-oriented sample spinning (MAOSS): A new approach toward biomembrane studies, *J. Magn. Reson.* **130,** 305–316 (1998).
47. M. E. Stoll, A. J. Vega, and R. W. Vaughan, Heteronuclear dipolar modulated chemical shift spectra for geometrical information in polycrystalline solids, *J. Chem. Phys.* **65,** 4093–4098 (1976).
48. R. K. Hester, J. L. Ackerman, B. L. Neff, and J. S. Waugh, Separated local field spectra in NMR: Determination of structure of solids, *Phys. Rev. Lett.* **36,** 1081–1083 (1976).
49. M. G. Taylor, T. Akiyama, and I. C. P. Smith, The molecular dynamics of cholesterol in bilayer membranes: a deuterium NMR study, *Chem. Phys. Lipids* **29,** 327–339 (1981).
50. R. L. Vold and R. R. Vold, Nuclear magnetic relaxation in coupled spin systems, *Prog. NMR Spectr.* **12,** 79–133 (1978).